AIAA JOURNAL
Vol. 39, No. 9, September 2001

k–ϵ Model for Predicting Transitional Boundary-Layer Flows Under Zero-Pressure Gradient

Seong Gu Baek* and Myung Kyoon Chung†
Korea Advanced Institute of Science and Technology, Taejon 305-701, Republic of Korea
and
Hyo Jae Lim‡
Hoseo University, Asan, Republic of Korea

A modified k–ϵ model is proposed for calculation of transitional boundary-layer flows. To develop the eddy viscosity model for the problem, the flow is divided into three regions: the pretransition region, transition region, and fully turbulent region. In the pretransition region, because the turbulence does not yet attain its equilibrium state in which the eddy viscosity is proportional to the distance from the wall, it is postulated that a viscous sublayer structure prevails across the boundary layer so that the eddy viscosity is proportional to the cube of the wall distance. Further it is assumed that as the turbulent spots which have appeared at the onset of transition grow with the downstream distance in the transition region, dependence of the eddy viscosity on the wall distance changes gradually from that in the pretransition region to that in the fully turbulent state. A universal downstream variation of intermittency factor in the transition region is employed to represent such a transition eddy viscosity in the transition region. In addition, the model constant $C_{\epsilon 1}$ in the standard k–ϵ model is modified to take into account the particular characteristics of turbulence in the transition region. In the present test calculations, because the governing equations are integrated from a point close to the leading edge in the pretransition region, the initial and boundary conditions of k and ϵ at the onset of transition are automatically supplied. The proposed model is applied to calculate three benchmark cases of the transitional boundary-layer flows with different freestream turbulent intensity (1–6%) under zero-pressure gradient. It was found that the profiles of mean velocity and turbulent intensity, local maximum of velocity fluctuations, their locations as well as the streamwise variation of integral properties such as skin friction, shape factor, and maximum velocity fluctuations are very satisfactorily predicted throughout the flow regions.

I. Introduction

In the past aerodynamic researches on the laminar-turbulent transition problem, most attention has been paid to predicting the onset point of transition rather than to investigating the transitional flowfield properties. But with such limited information transitional boundary-layer flows are difficult to predict in many applications such as the internal flows in axial turbomachinery where the blade transitional boundary layer occupies 40–80% of chord length,[1] where freestream turbulence intensity is very high and where the pressure gradient varies along the surface. A consequent large variation of skin friction in such an extended length of transition region affects the overall performance of turbomachinery. Especially when the freestream turbulence intensity is high, the velocity fluctuations caused by disturbances within the boundary layer interact with freestream turbulence, and their amplitude grows rapidly downstream. The linear instability process caused by to natural transition is bypassed, and only the nonlinear instability process prevails in the pretransition region (from the leading edge to the onset of transition), which is often called the "bypass transition." The present study is aimed at predicting the transitional boundary layer caused by the bypass transition under high freestream turbulent intensity.

Zero-equation turbulence models[2] frequently have been used in the calculation of turbulent boundary layers including transition. However, such models cannot describe the turbulent flow structure in the transitional boundary-layer flows. In contrast, the one-equation models[3] give the information about the fluctuation scale in the flows. Both types of turbulence models use the intermittency factor as a corrective function to the eddy viscosity in the transition region. In 1991–1993 the Ercoftac Special Interest Group examined various turbulence models to compare their performance in predicting the downstream variation of skin friction in the bypass transition problem.[4] They concluded that in order to correctly predict the properties in the transitional boundary layer special treatment was needed in turbulence models and that even the Launder and Sharma's[5] model, which was found as the best performer in the category of two-equation turbulence models, gave unsatisfactorily too early transition onset point and too short transition length. In addition, its prediction performance was found to depend on the initial conditions at the leading edge. One of the reasons for the incapability of two-equation models was attributed to the anisotropy of turbulence that cannot be described by the models. However, even with Reynolds-stress models that explicitly treat the anisotropy of turbulence, the predictions still fell short of expectation.[4,6] After 1990 the ever-increasing need for correct prediction of transitional boundary-layer flows leads to several developments of specialized computational models for this problem. Young et al.[7] adopted a laminar length scale and a velocity jump in modeling the Reynolds shear stress in the transition region. Steelant and Dick[8] evaluated a conditioned average equation for transitional boundary layer. They devised a differential equation of the intermittency factor that was derived from an empirical correlation of streamwise intermittency variation. Savill[9] developed a Reynolds-stress transport model, the Savill–Launder–Younis-γ model, where a modified Cho and Chung's[10] differential intermittency equation was adopted. He showed that SLY-γ model yields reasonable predictions of velocity fluctuations in the pretransition region and the skin friction in the transition region.

Scrutinizing all of the existing models that have been used to analyze the transitional boundary-layer problem, it was found that the relevant physics of transition have not been taken into account in the modeling process. Only one exception is, to the best knowledge of the present authors, Mayle and Schulz[11] who paid their attention to the pressure fluctuation term in the kinetic energy equation that was considered as a driving force to amplify disturbances in the pretransition region. Receptivity (that is the transformation of

Received 23 October 2000; revision received 1 January 2001; accepted for publication 15 January 2001.

*Graduate Assistant, Department of Mechanical Engineering.
†Professor, Department of Mechanical Engineering; mkchung@cais.kaist.ac.kr.
‡Professor, Division of Mechanical Engineering.

external disturbances into internal ones in the vicinity of the leading edge) is also included in their kinetic energy equation model. Their model showed some improvement in predicting the pretransition region; however, it failed to calculate the transition region with reasonable accuracy.

The main objective of the present study is to develop a new turbulence model that can be used to calculate the whole transitional boundary-layer flow which consists of pretransition region, transition region, and the fully turbulent region. First, the eddy viscosity model in the pretransition region is derived based on the physics in the pretransition region. Second, because the transition region bridges the pretransition region upstream and the fully turbulent one downstream, it is assumed that a smoothly bridging function in terms of the local mean intermittency factor can be used to model the downstream variation of the eddy viscosity in the transition region. Details of the modeling procedure are described in the Secs. II and III, and sample calculations are given in Sec. IV to test the prediction performance of the new k–ϵ model developed in this study.

II. Modeling of Reynolds Shear Stress

In intermittent turbulent flows the Reynolds shear stress is represented by[1]

$$\overline{u_i u_j} = \gamma \overline{\widetilde{u_i u_j}} + (1-\gamma)\overline{\widetilde{u_i u_j}} + \gamma(1-\gamma)\Delta U_i \Delta U_j \qquad (1)$$

where $\overline{\widetilde{\ }}$ and $\overline{\widetilde{\ }}$ denote the turbulent and the nonturbulent zone averages, respectively. $\Delta U_i = \overline{\widetilde{U_i}} - \overline{\widetilde{U_i}}$ is the "velocity jump" that represents the mean velocity difference between turbulent and nonturbulent part at the same location. When $i = j$, this jump contributes significantly to the increase in the normal stress so that the anisotropy prevails in the transition region, but in the case of shear stress when $i \neq j$ its contribution to the shear stress is negligible.[12] Experimentally, it is known that the fluid particles in a turbulent spot are in a fully turbulent state and that most of the spots are generated at the point of transition onset and grow with the downstream distance until merging into a fully turbulent flow region. Therefore, the frequency of appearance of turbulent spots at a point in space is closely associated with the intermittency factor at that point, and the local intermittency seems to be nearly proportional to the average across the stream. Therefore, it may be assumed that

$$\gamma(x, y) = \gamma_x \cdot \gamma_y \qquad (2)$$

in the transitional boundary layer. Here, γ_x is the streamwise variation of the near-wall intermittency, and γ_y is a representative vertical profile of intermittency. Then, substituting this assumption into Eq. (1), it follows that

$$\overline{u_i u_j} \approx \gamma_x \underbrace{\left\{\gamma_y \overline{\widetilde{u_i u_j}} + (1-\gamma_y)\overline{\widetilde{u_i u_j}}\right\}}_{\text{Eddy viscosity}} + (1-\gamma_x)\overline{\widetilde{u_i u_j}} (i \neq j) \qquad (3)$$

Pretransition Region (PTR)

Although there are some fluctuations in the streamwise velocity,[11] no turbulent spot exists in the pretransition region so that $\gamma_x = 0$, and only the last term of right-hand side of Eq. (3) remains to be nonzero. Then, to keep the analogy with the turbulent eddy viscosity model in modeling the PTR Reynolds shear stress, we assume that

$$-\overline{u_i u_j} = -\overline{\widetilde{u_i u_j}} = 2\nu_{\text{PTR}} S_{ij} \qquad (i \neq j) \qquad (4)$$

where $S_{ij} = \frac{1}{2}(U_{i,j} + U_{j,i})$ and $\nu_{\text{PTR}} = [V]_{\text{PTR}}[L]_{\text{PTR}}$. $[V]_{\text{PTR}}$ and $[L]_{\text{PTR}}$ represent appropriate velocity and length scales that are related to the momentum transfer in the pretransition region, respectively. Here, we can simply choose $\sqrt{k}$ as the PTR velocity scale like that in the fully turbulent region. But in determining a $[L]_{\text{PTR}}$ a rather crude assumption is made because relevant information is difficult to experimentally collect within the extremely thin boundary layer in the PTR. It is reasoned that the fully turbulent flow region is characterized by the appearance of the logarithmic equilibrium layer where the eddy viscosity is proportional to the distance from the wall. Also note that the eddy viscosity in very-near-the-wall layer in fully turbulent flows is proportional to third power of the wall distance.[13] Therefore, because the equilibrium logarithmic layer does not yet appear in the PTR, viscous sublayer structure may prevail across the boundary layer in the PTR, and consequently the PTR eddy viscosity is assumed to be proportional to the cube of the wall distance. From this reasoning we propose the following model:

$$\nu_{\text{PTR}} = C_{\text{PTR}}(\nu/u_\tau)\sqrt{k}y^{+2} \qquad (5)$$

where C_{PTR} is a model constant and recall that k is proportional to the squre of y near the wall. At the boundary-layeredge in the PTR, it follows that

$$C_{\text{PTR}} \sim k_\infty^{+\frac{3}{2}} \Big/ \delta_\infty^{+2}\epsilon_\infty^{+} \qquad (6)$$

where δ_∞^+ is the dimensionless boundary-layer thickness and k_∞^+ and ϵ_∞^+ are the freestream values of the turbulent kinetic energy and its dissipation rate normalized by the viscous wall scale. Hence C_{PTR} is dependent on the freestream condition. The functional dependence is still in scrutiny. Compared with Mayle and Schulz's[11] model, C_{PTR} corresponds to C_ω, which depends on the freestream near the leading edge.

Transition Region

Because $\gamma_x \neq 0$ here, the eddy viscosity (EV) part in Eq. (3) must be modeled. Consider the case $\gamma_x = 1.0$. Then the EV part becomes equal to the conventional Reynolds shear stress. The nonturbulent shear stress in the EV part is different from that in the pretransition region. A number of flow visualizations[14,15] reveal that the latter stems from the downstream movement of nonturbulent fluid particles, whereas the former is caused by both the turbulent spots and the entrainment of irrotational freestream fluids into the boundary layer at its edge. Further consideration that the fluid in turbulent spots is in fully turbulent state leads one to conclude that the rate of momentum transfer as a result of the EV part in the transition region is proportional to the mixing level of the turbulent spots with the remaining nonturbulent fluids. Therefore, we can assume the following model:

$$\text{EV} = 2 f_{\text{mix}} \nu_T S_{ij} \qquad (i \neq j) \qquad (7)$$

where ν_T is the conventional eddy viscosity model for fully turbulent flows and f_{mix} represents the relative mixing level of turbulent spots. Obviously the latter has the value of unity in turbulent flows. In many previous transition models a simple model $f_{\text{mix}} = 1$ was frequently used.[2,3,7] However, it gives faster growth of skin friction and shorter transition length compared to experimental data. Sharma[16] suggested that a first-order function of γ_x must be used to reduce the discrepancy. Because the volume of fluid particles in fully turbulent state is assumed to be proportional to γ_x^3, a third-order function of γ_x in the following form was chosen to represent the relative mixing level:

$$f_{\text{mix}} = C_{\text{mix}} + (1.0 - C_{\text{mix}})\gamma_x^3 \qquad (8)$$

where C_{mix} is a constant to be determined later in the result and discussion section. Finally, models of Eqs. (5) and (7) lead to the following final form:

$$-\overline{u_i u_j} = \nu_{\text{TR}} S_{ij} \qquad (i \neq j) \qquad (9)$$

where

$$\nu_{\text{TR}} = \gamma_x f_{\text{mix}} \nu_T + (1-\gamma_x)\nu_{\text{PTR}} \qquad (10)$$

This implies that at least two length scales are present in the transitional boundary layer, which has been proved theoretically by Volino and Simon[17] and experimentally by Blair[12] and Wang and Zhou.[18]

Now consider the functional form of γ_x. It was found by an experimental study that, in transition region, γ_x has a universal profile that is independent of the freestream turbulence intensity and the pressure gradient.[19] And its empirical correlation was found by various experiments[20] in the following form:

$$\gamma_x = \begin{cases} 0 & \text{if} \quad Re_x < Re_{xt} \\ 1 - \exp\left[-\hat{n}\sigma(Re_x - Re_{xt})^2\right] & \text{if} \quad Re_x \geq Re_{xt} \end{cases} \qquad (11)$$

where $\hat{n}\sigma$ is defined as a spot formation rate and subscript xt denotes the transition onset point. These are dependent on the freestream turbulence and the pressure gradient. Under zero-pressure gradient, their correlations are as follows[1]:

$$\hat{n}\sigma = 1.5 \times 10^{-11} Tu_t^{\frac{7}{4}} \tag{12}$$

$$Re_{\theta t} = 420 Tu_t^{-0.69} \tag{13}$$

where Tu_t and subscript θt denote the freestream turbulence intensity and the momentum thickness at the transition onset point, respectively. Here, Re_{xt} is the Reynolds number at the point where the momentum thickness Reynolds number satisfies Eq. (13).

III. Turbulent Kinetic Energy and Its Dissipation Rate Equations

For a steady incompressible flow the exact equation governing the transport of k is

$$U_j \frac{\partial k}{\partial x_j} = D_k + T_k + \Pi_k + P_k - \epsilon \tag{14}$$

where

$$D_k = \nu k_{,jj}, \qquad T_k = -\overline{(u_j k)}_{,j}, \qquad \Pi_k = (1/\rho)\overline{(u_j p)}_{,j}$$

$$P_k = -\overline{u_i u_j} S_{ij}, \qquad \epsilon = \nu \overline{u_{i,j} u_{i,j}}$$

The production term P_k is evaluated with the Reynolds shear-stress model developed in Sec. II, and the turbulent transport term T_k is assumed to be the same as that in fully turbulent flows. The viscous diffusion term is evaluated exactly. Now consider the pressure diffusion term. By Voke and Yang's[21] LES data on the normal stress budget downstream and their transition scenario, the pressure diffusion term Π_k is negligibly small in both the pretransition and transition regions. It is only in the vicinity of leading edge where the term exhibits nonnegligible values. Therefore it affects the receptivity mechanism that initial disturbances are generated and amplified near the leading edge. Because, however, its effects have not been quantitatively well understood, its direct modeling is omitted in the present study. As the fluid flows downstream, it is the Reynolds shear stress (via eddy viscosity) that directly affects the growth of disturbance amplitude. By a small adjustment of the model constant in the turbulent transport term that is to be modeled with the eddy viscosity, the effect of the pressure diffusion term may be taken into account in the turbulent transport term. The preceding modeling strategy yields the following model equation of the turbulent kinetic energy:

$$\frac{Dk}{Dt} = \frac{\partial}{\partial y}\left[\left(\nu + \frac{\nu_{TR}}{\sigma_k}\right)\frac{\partial k}{\partial y}\right] + P_k - \epsilon \tag{15}$$

where

$$P_k = \nu_{TR}\left(\frac{\partial U}{\partial y}\right)^2 - (\overline{u'^2} - \overline{v'^2})\frac{\partial U}{\partial x} \tag{16}$$

Here the difference of normal stresses is modeled as

$$\overline{u'^2} - \overline{v'^2} = C_{uv} k \tag{17}$$

When $\gamma_x = 1.0$ in fully turbulent flow, C_{uv} must be about 0.33, and when $\gamma_x = 0$ in the pretransition region, $u'^2 \gg v'^2$, then $\overline{u'^2} \approx 2k$. Several simple correlations satisfying these two extremes have been tested, and a good approximate function was found to have the following form:

$$C_{uv} = 0.33 + 1.67\left(1 - \gamma_x^3\right) \tag{18}$$

As for ϵ equation, the conventional ϵ equation of the two-equation model is used with ν_T replaced by ν_{TR} as follows:

$$\frac{D\epsilon}{Dt} = \frac{\partial}{\partial y}\left[\left(\nu + \frac{\nu_{TR}}{\sigma_\epsilon}\right)\frac{\partial \epsilon}{\partial y}\right] + C_{\epsilon 1}^* f_1 \frac{\epsilon}{k} P_k - C_{\epsilon 2} f_2 \frac{\epsilon^2}{k} + E \tag{19}$$

In the standard k–ϵ model the second term in the right-hand side in Eq. (19) is employed to keep the turbulent kinetic energy from growing indefinitely as a result of the production of turbulence. And its model constant $C_{\epsilon 1}$ is determined to secure the logarithmic equilibrium layer with the von Karman constant of 0.41. However, there is no such equilibrium layer in the transition region, and therefore the conventional value of $C_{\epsilon 1}$ should be modified in order to represent the particular nature of turbulence in this region. As already mentioned, the streamwise velocity begins to fluctuate in the PTR that is not associated with dissipation mechanism of any noticeable magnitude. This implies that the turbulent kinetic energy has grown excessively up to the point of transition onset. Therefore it is necessary to strongly damp the growing of turbulence for a while soon after the advent of turbulent spots, which means that a larger value than the conventional one must be assigned to $C_{\epsilon 1}$ in the transition region. Here again a number of trials with various functional correlations for $C_{\epsilon 1}$ have been made, and the following form was found to reasonably reproduce the growth of local maximum of streamwise fluctuations in the transition region:

$$C_{\epsilon 1}^* = C_{\epsilon 1}\left\{1 + 0.1\left(1 - \gamma_x^2\right)H(\gamma_x)\right\} \tag{20}$$

Here, H is a Heaviside step function, and the model constants C_μ, $C_{\epsilon 1}$, $C_{\epsilon 2}$ depend on the selection of standard turbulence model. The last term E depends on the choice of the low-Reynolds-number k–ϵ model. For example, $E = \gamma_x f_{\text{mix}} \nu \nu_T (\partial^2 U/\partial y^2)^2$ in Yang and Shih's[22] model $E = 0$ in Nagano and Tagawa's[23] model. Here, $\gamma_x f_{\text{mix}} \nu_T$ is the turbulent portion of eddy viscosity in transition region. In the pretransition region the ν_{TR} term becomes ν_{PTR}, and the E term vanishes because γ_x goes to zero. And the damping functions based on fully turbulent flows must be modified to represent the characteristics of transitional flows. In this case $f_1 = f_{PTR1} = 0.9$ and $f_2 = f_{PTR2} = 1 - \exp(-y^{+2})$ were chosen to give the best prediction of growth rates of local maximum fluctuation of u' in the pretransition region and to satisfy the wall behavior of the ϵ equation. Here, because the k and ϵ do not have any similarity in the pretransition region unlike in fully turbulent flows, the local turbulent quantities using k, ϵ such as Re_T, Re_y, etc., must be avoided in choosing the functional variable for damping in the pretransition region. The boundary condition for ϵ on the wall in PTR is determined by applying Eq. (15) at the wall, which gives

$$\epsilon_{w\text{PTR}} = \nu k_{,yy} \tag{21}$$

In the transition region the turbulent spots in which the state of turbulence is of a fully evolved one prevail, and the accelerated growth of dissipation mechanism in the initial transition region leads us to use the same damping functions f_1 and f_2, as those used in the fully turbulent region downstream. The wall condition for ϵ in the transition region is given by a conditioned average, which is

$$\epsilon_{w\text{TR}} = \gamma_x \epsilon_{wT} + (1 - \gamma_x)\epsilon_{w\text{PTR}} \tag{22}$$

IV. Results and Discussion

The model equations were solved with a parabolic boundary-layer code EDDYBL of Wilcox.[13] The detailed information of the code is provided in Ref. 13. The inflow conditions to the pretransition region was given at 10 mm downstream of the plate leading edge with the following profiles:

$$k = k_0\left(\frac{U}{U_\infty}\right)^2, \qquad \epsilon = \max\left\{\epsilon_0; 0.3k\left|\frac{\partial U}{\partial y}\right|\right\} \tag{23}$$

where $\epsilon_0 = k_0^{3/2}/l_{\epsilon 0}$ and k_0 and $l_{\epsilon 0}$ are the turbulent kinetic energy and dissipation length scale of the freestream turbulence, respectively. The turbulent kinetic energy k_0 was given by the freestream turbulence level at the starting x position and dissipation length $l_{\epsilon 0}$ was chosen to fit the experimentally determined decay curve of the freestream turbulence. To integrate the equations right from the wall boundary, a low-Reynolds-number k–ϵ turbulence model must be used. In the present study Nagano and Tagawa's [23] model and Yang and Shih's[22] model were chosen because they all use ϵ defined in its standard form in k and ϵ equation. Nagano and Tagawa's model is a widely used model in industrial applications, and Yang and Shih's model has been developed based on DNS data.

Three test cases (J. Coupland, Applied Science Lab., Rolls–Royce, Derby, England, United Kingdom, Dec. 1993, private communication) were computed in the present paper. All of them

are transitional boundary-layer flows on a flat plate with a sharp leading edge under zero-pressure-gradient condition. These experiments have been taken as standard transitional flows.[4] The test cases are denoted as T3AM ($Tu = 1.0\%$, $U_\infty = 19.8$ m/s), T3A ($Tu = 3.0\%$, $u_\infty = 5.2$ m/s) and T3B ($Tu = 6.0\%$, $U_\infty = 9.4$ m/s). Here Tu denotes the freestream turbulence intensity at the leading edge. Because the model constant C_{PTR} depends on the freestream turbulence conditions, appropriate value must be obtained directly from experimental data. The value of C_{PTR} used in the present computations are 3.0×10^{-5} for T3AM, 3.0×10^{-4} for T3A, and 6.0×10^{-4} for T3B, respectively. Further the model constant C_{mix} in Eq. (8) for f_{mix} depends on the choice of turbulence model because it is related to the damping function f_μ, of which form is dependent on the turbulence model used. The functional form of C_{mix} is

$$C_{\mathrm{mix}} = C_{\mathrm{TM}} \cdot Tu_t^{0.7}$$

where C_{TM} is a model constant and Tu_t is the freestream turbulent intensity at the transition onset. C_{TM} is 0.16 for Nagano and Tagawa's model and 0.10 for Yang and Shih's model. C_{mix} dictates the relative initial growth of turbulent phase at the transition onset. Low-Reynolds-number models of Yang and Shih and Nagano and Tagawa were tested in the present study. The prediction with Nagano and Tagawa's model gave a little better prediction of the growth rate of skin-friction coefficient (not shown); however, both models yield nearly identical predictions in most cases, and the following results are the predictions with Yang and Shih's model.

Figure 1 shows mean velocity profiles in the transition region. Mean velocity profiles in the pretransition region are almost the

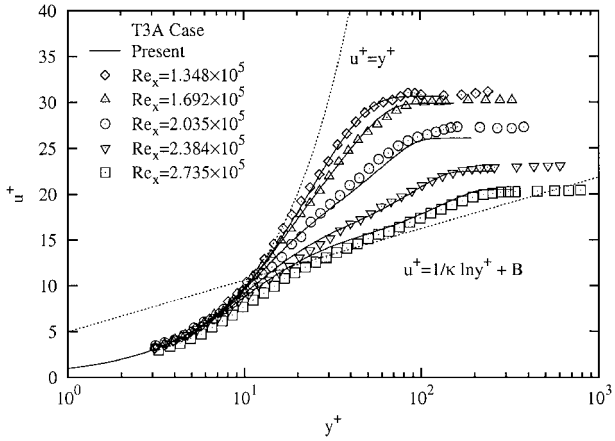

a) T3A case

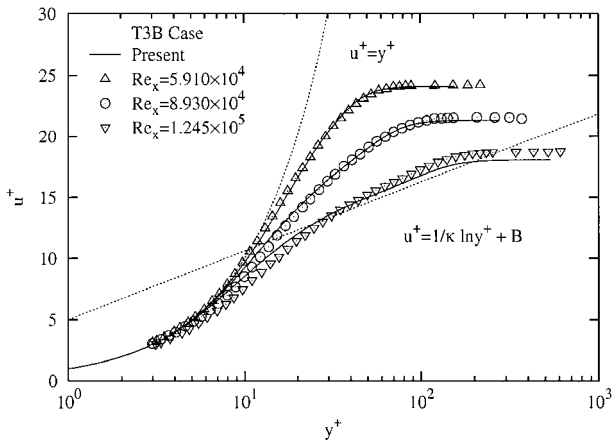

b) T3B case

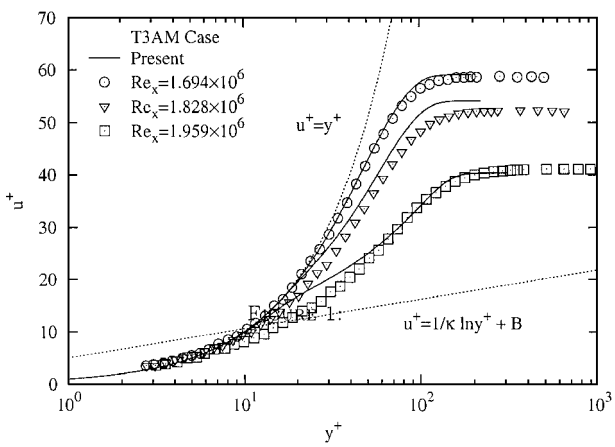

c) T3AM case

Fig. 1 Comparison of computed mean velocity profiles with measurements in transition region.

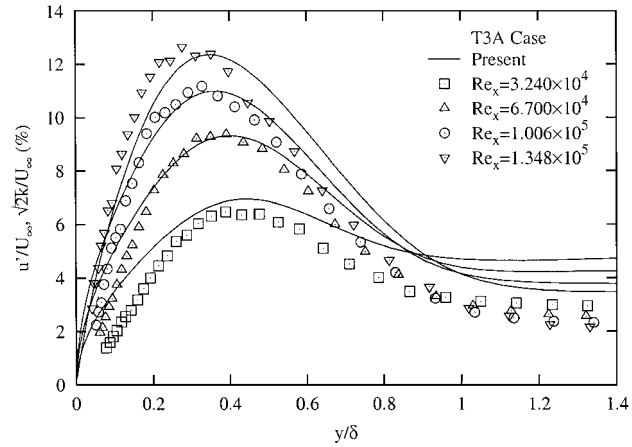

a) T3A case

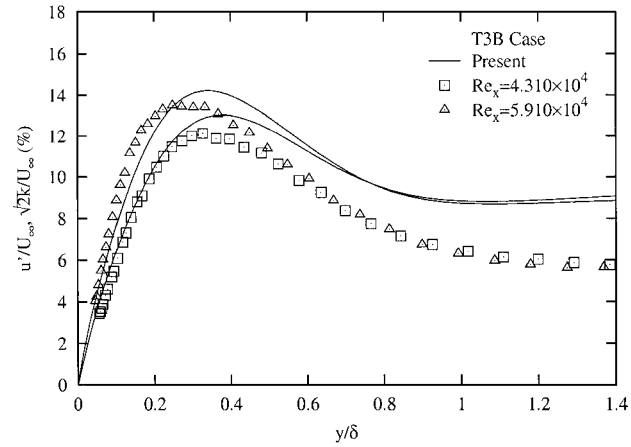

b) T3B case

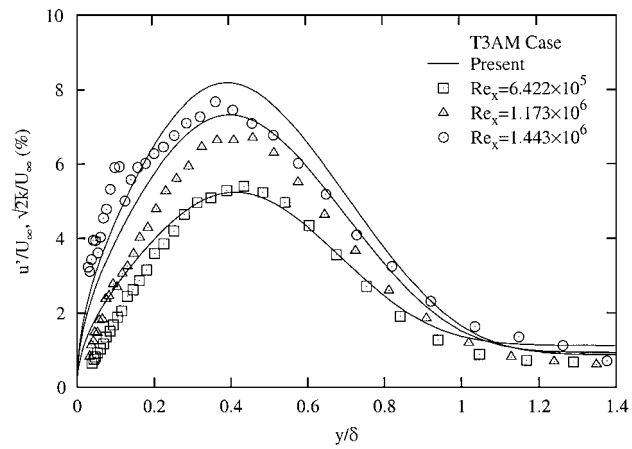

c) T3AM case

Fig. 2 Comparison of computed turbulent intensity with measured profiles of streamwise velocity fluctuation component in pretransition region.

same as the Blasius similarity solution and are not shown here. For example, in the case of T3A all pretransition mean velocity profiles are nearly same as the profile at $Re_x = 1.348 \times 10^5$ in Fig. 1a. Also, there appears a profile in each case where the freestream mean velocity is different between the experiment and the prediction. The reason is not clearly understood. It may be caused by the difficulty in experimentally maintaining the freestream velocity constant throughout the measurement. Besides this difference, the computational results are in very good agreement with experimental data.

Figure 2 shows the velocity fluctuation profiles in the pretransition region. Streamwise velocity fluctuation u'_{rms} of experimental data and the computed turbulent kinetic energy $\sqrt{2k}$ are compared. In the pretransition region experimental measurements reveal that the streamwise fluctuation component is predominantly larger than the normal and crossflow components so that it is possible to approximate as $\sqrt{2k} \approx u'_{\text{rms}}$. The present model gives very good prediction of the fluctuation profiles. Especially the predicted locations of maximum fluctuations and its values are far better than those of Mayle and Schulz's model, which predicts the peak of the profiles much closer to the wall than the measurements. In all three test cases the fluctuations are overpredicted by about 20% in the wall region, $y/\delta < 0.1$. This is caused by the inability of our model to capture the immature streaky structure near the wall at low Reynolds number. In spite of these discrepancies, the agreement between the calculated and the measured profiles is remarkable.

The profiles of streamwise rms velocity in the transition region are shown in Fig. 3. Again, the predicted profiles are those of $\sqrt{2k}$. The streamwise location of the profiles is at the position where the local maximum of the streamwise rms velocity profile along the y direction attains its maximum value during the laminar-turbulent transition. In case T3A, the calculated $\sqrt{2k}/U_\infty$ is larger by about 40% than the measured u'_{rms}/U_∞, 20% for T3B, and about 50% for T3AM in the core region, $0.2 < y/\delta < 0.8$. Experimental data show that $v'_{\text{rms}} \approx 0.5u'_{\text{rms}}$ and $w'_{\text{rms}} \approx 0.5u'_{\text{rms}}$ in the core of the boundary layer. Therefore we have

$$2k = \overline{u'^2} + \overline{v'^2} + \overline{w'^2} \approx 1.5\overline{u'^2}$$

Then, $\sqrt{2k} \approx 1.2u'_{\text{rms}}$. From this it can be deduced that the difference between the calculated and the measured values is nearly negligible for T3B; it is about 20% for T3A and about 30% for T3AM. It is found that the discrepancy increases with decreasing freestream turbulent intensity. Especially in $y/\delta < 0.2$ of case T3AM where the freestream turbulence intensity is relatively low, it was underpredicted by about 50%. Considering the fact that the anisotropy in Reynolds normal stresses is strong and the natural instability prevails under a low freestream turbulence intensity where Tollmien–Schlichting frequency is detected, such discrepancy is attributed to the basic assumptions of bypass transition and weak anisotropy under which the present model has been formulated.

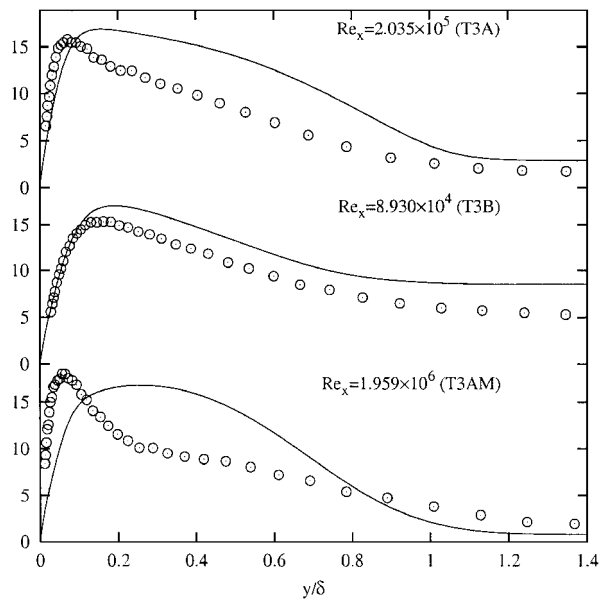

Fig. 3 Profiles of computed turbulent intensity with measured streamwise velocity fluctuation component in transition region at position where the local maximum of u'_{rms} has the maximum: ——, calculated $\sqrt{2k}$ and ∘, measured u'_{rms}.

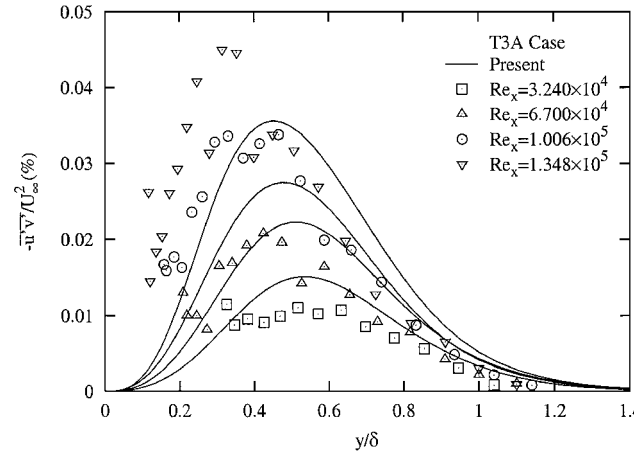

a) T3A case

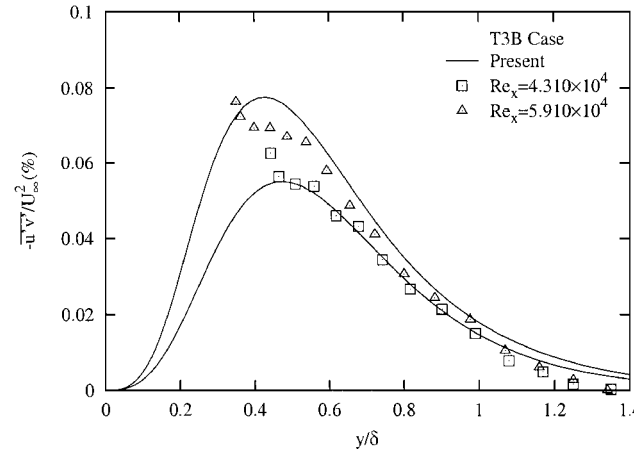

b) T3B case

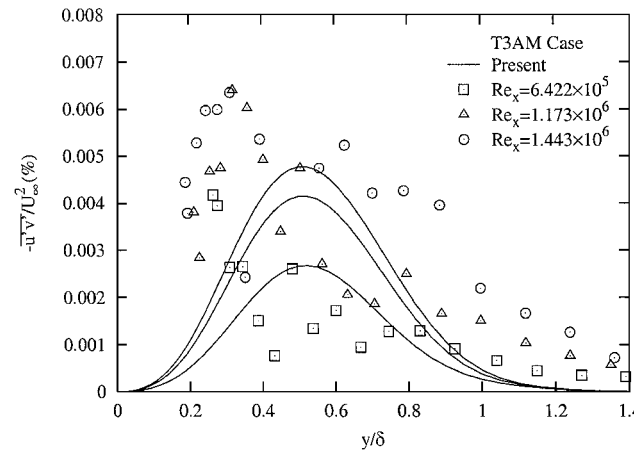

c) T3AM case

Fig. 4 Profiles of computed Reynolds shear stress with measurements in pretransition region.

Figure 4 displays the Reynolds shear-stress profiles in the pretransition region. Although the experimental data scatter very widely, Fig. 4a of case T3A and Fig. 4b of case T3B show that the location of maximum Reynolds shear stress and its value are reasonably predicted. Also from Fig. 4c of case T3AM with even wider scatter of the experimental data, it may be found that the tendency of the

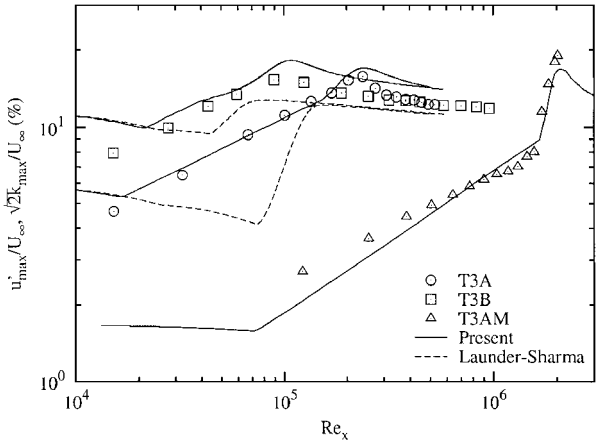

Fig. 5 Growth rates of the local maximum of u'_{rms}.

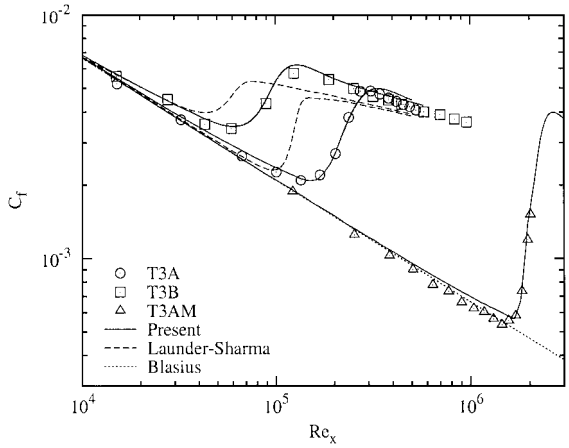

Fig. 6 Comparison of computed variation of skin friction with measurements.

growth of the Reynolds shear stress downstream is to some extent in coincidence with the measurement.

Figure 5 compares the predicted growth of maximum value of the streamwise velocity fluctuations with those of Launder and Sharma's model. In cases T3A and T3B the linear growth is well predicted. But, for case T3AM, while the maximum value grows linearly with Reynolds number, the growth is somewhat steeper than the experimental data. Especially in the transition region the rapid increase of the streamwise velocity fluctuations is nicely captured to its maximum point.

Figure 6 displays the predicted and measured skin-friction coefficients. Predictions by using the Launder and Sharma's model and the Blasius profile $C_f = 0.664 Re_x^{-1/2}$ are also included for comparison. As can be seen, the present predictions of the point of transition onset, transition length, and its rate of increase during the transition are in almost perfect agreement with experiments, whereas the Launder and Sharma's model, which has been known as the best model among all available two-equation models for analysis of transitional flows, yields too early onsets of transition and shorter transition lengths.

Finally a comparison between predicted and measured shape factors is shown in Fig. 7. It has been known that the shape factor is 2.6 for a laminar boundary layer and 1.4 for a turbulent boundary layer. However, both the predictions and the experiments reveal that the shape factor decreases nearly linearly in the pretransition region (or conventionally called "laminar boundary layer") under strong freestream turbulence intensity like cases T3A and T3B. This suggests that an effective eddy viscosity model such as the present PTR Reynolds-stress model must be employed even in the pretransition region. But in the case T3AM the shape factor remains constant in the pretransition region, and it was underpredicted by about 4%. It begins to decrease right before the transition onset. The discrepancy between the prediction and the measurement for this case arises from

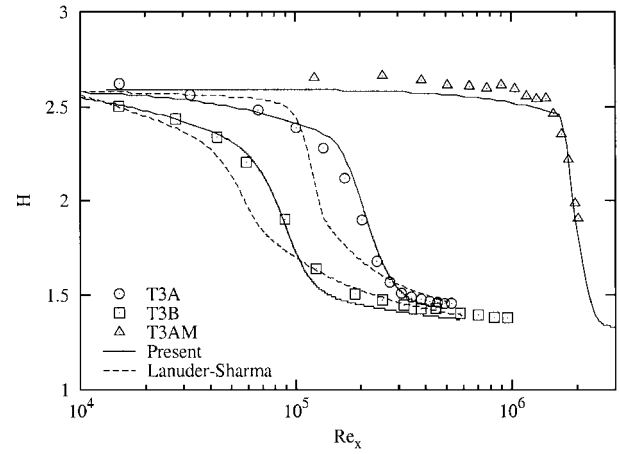

Fig. 7 Downstream variation of computed and measured shape factors.

the fact that case T3AM is close to the natural transition, which is caused by Tollmien–Schlichting wave.

V. Conclusions

A new k–ϵ model has been proposed for an analysis of boundary-layer flows including transition phenomenon under appreciable freestream turbulence intensity. To develop the model equations, the transitional boundary layer is divided into three regions according to their physical characteristics, namely, pretransition region, transition region, and fully turbulent region. In the pretransition region it is postulated that the turbulence does not yet attain its equilibrium state in which the eddy viscosity is proportional to the distance from the wall, and thus viscous sublayer structure prevails across the boundary layer so that the eddy viscosity is proportional to the cube of the wall distance. At the onset of transition, the turbulent spots appear, and the volume of the spots grow with the downstream distance. Along with the development of small-scale eddies and with the mixing between the turbulent spots and the nonturbulent fluid particles with the downstream distance, the wave number of the energy-containing eddies shifts from low- to high-wave-number range so that two different scales switch over their significance in maintaining the turbulence structure in the transition region: one is the molecular scale pertaining to the pretransition region, and the other is the turbulent scale in the fully turbulent region. Consequently, two length scales must be employed simultaneously to describe the transient behavior in the transition region. To bridge the two length scales pertinent to the two extremes, one upstream and the other downstream, a universal model of streamwise variation of the intermittency factor was employed, which represents the relative mixing level of the turbulent spots in the transition region.

Three benchmark transitional flows under zero-pressure gradient with high freestream turbulent intensity ($Tu = 1$–6%) were computed with the present model, and their results were compared with both experimental data and predictions by using the Launder and Sharma's model that has been assessed as one of the best two-equation models for analysis of transitional flows. Profiles of mean velocity, streamwise turbulent velocity fluctuations and Reynolds shear stresses, and streamwise variations of local maximum streamwise rms velocity, skin friction and the shape factor are compared between predictions and the measurements. It was found that the present model predicts satisfactorily the mean flowfield as well as the turbulent properties throughout the transitional boundary layer. Among the three cases, the one with lowest freestream turbulent intensity was predicted with lesser accuracy by the present model, which is attributed to the linear instability problem inherent in the transition caused by the Tollmien–Schlichting wave. Even in this case, however, all flow properties are predicted with better accuracy by the present model in comparison with that of Launder and Sharma.

Further investigation is needed to include the pressure gradient effect in the present model equations to calculate the transition problem. Also important is to find a robust low-Reynolds-number

k–ϵ turbulence model to which the present modifications are adapted in order to analyze the transitional boundary layer in a wider range of flow conditions.

Acknowledgments

This work was supported by a grant from the National Research Laboratory program of the Ministry of Science and Technology of Korea and by Grants 98-0200-1201-3 and 95-0200-1601-3 from the Basic Research Programs of Korea Science and Engineering Foundation. Especially, the authors express special thanks to the latter organization for its continuing support.

References

[1]Mayle, R. E., "The Role of Laminar–Turbulent Ttransition in Gas Turbine Engines," *Journal of Turbomachinery*, Vol. 113, Oct. 1991, pp. 509–537.

[2]Cebeci, T., and Smith, A. M. O., *Analysis of Turbulent Boundary Layers,* Academic Press, New York, 1974, pp. 234–239.

[3]Rodi, W., Mansour, N. N., and Michelassi, V., "One-Equation Near-Wall Turbulence Modeling with the Aid of Direct Simulation Data," *Journal of Fluid Engineering*, Vol. 115, June 1993, pp.196–205.

[4]Savill, A. M., "A Summary Report on the COST ERCOFTAC Transition SIG Project Evaluating Turbulence Models for Predicting Transition," *ERCOFTAC Bulletin*, Vol. 24, March 1995, pp. 54–67.

[5]Launder, B. E., and Sharma, B., "Application of the Energy Dissipation Model of Turbulence to the Calculation of Flow near a Spinning Disc," *Letters in Heat and Mass Transfer*, Vol. 1, No. 2, 1974, pp. 131–138.

[6]Westin, K. J. A., and Henkes, R. A. W. M., "Application of Turbulence Models to Bypass Transition," *Journal of Fluids Engineering*, Vol. 119, Dec. 1997, pp. 859–866.

[7]Young, T. W., Warren, E. S., Harris, J. E., and Hassan, H. A., "New Approach for the Calculation of Transition Flows," *AIAA Journal*, Vol. 31, No. 4, 1993, pp. 629–636.

[8]Steelant, J., and Dick, E., "Modeling of Bypass Transition with Conditioned Navier–Stokes Equations Coupled to an Intermittency Transport Equation," *International Journal of Numerical Methods in Fluids*, Vol. 23, 1996, pp. 193–220.

[9]Savill, A. M., "One-Point Closures Applied to Transition," *Turbulence and Transition Modelling*, edited by M. Hallbäck, D. S. Hemmingson, A. V. Johansson, and P. H. Alfredsson, Kluwer Academic, Norwell, MA, 1996, pp. 233–268.

[10]Cho, J. R., and Chung, M. K., "A k–ϵ–γ Equation Turbulence Model," *Journal of Fluids Mechanics*, Vol. 237, April 1992, pp. 301–322.

[11]Mayle, R. E., and Schulz, A., "The Path to Predicting Bypass Transition," *Journal of Turbomachinery*, Vol. 119, July 1997, pp. 405–411.

[12]Blair, M. F., "Boundary-Layer Transition in Accelerating Flows with Intense Freestream Turbulence: Part 2—The Zone of Intermittent Turbulence," *Journal of Fluids Engineering*, Vol. 114, Sept. 1992, pp. 322–332.

[13]Wilcox, D. C., *Turbulence Modeling for CFD,* 2nd ed., DCW Industries, La Cañada, CA, 1998.

[14]Perry, A. E., Lim, T. T., and Teh, E. W., "A Visual Study of Turbulent Spots," *Journal of Fluids Mechanics*, Vol. 104, March 1981, pp. 387–405.

[15]Ducros, F., Comte, P., and Lesieur, M., "Large-Eddy Simulation of Transition to Turbulence in a Boundary Layer Developing Spatially over a Flat Plate," *Journal of Fluids Mechanics*, Vol. 326, Nov. 1996, pp. 1–36.

[16]Sharma, O. P., "Momentum and Thermal Boundary Layer Development on Turbine Airfoil Suction Surfaces," AIAA Paper 87-1918, 1987.

[17]Volino, R. J., and Simon, T. W., "An Application of Octant Analysis to Turbulent and Transitional Flow Data," *Journal of Turbomachinery*, Vol. 116, Oct. 1994, pp. 752–758.

[18]Wang, T., and Zhou, D., "Spectral Analysis of Boundary-Layer Transition on a Heated Flat Plate," *International Journal of Heat and Fluid Flow*, Vol. 17, No. 1, 1996, pp. 12–21.

[19]Dhawan, S., and Narashima, R., "Some Properties of Boundary Layer During the Transition from Laminar to Turbulent Flow Motion," *Journal of Fluids Mechanics*, Vol. 3, Pt. 4, Jan. 1958, pp. 418–436.

[20]Gostelow, J. P., Blunden, A. R., and Walker, G. J., "Effects of Free-Stream Turbulence and Adverse Pressure Gradients on Boundary Layer Transition," *Journal of Turbomachinery*, Vol. 116, July 1994, pp. 392–404.

[21]Voke, P. R., and Yang, Z., "Numerical Study of Bypass Transition," *Physics of Fluids*, Vol. 7, No. 9, 1995, pp. 2256–2264.

[22]Yang, Z., and Shih, T. H., "New Time Scale Based k–ϵ Model for Near-Wall Turbulence," *AIAA Journal*, Vol. 31, No. 7, 1993, pp. 1191–1198.

[23]Nagano, Y., and Tagawa, M., "An Improved k–ϵ Model for Boundary Layer Flows," *Journal of Fluids Engineering*, Vol. 112, March 1990, pp. 33–39.

R. M. C. So
Associate Editor